metals

Article

Metadynamic Recrystallization Behavior of Cr-Ni-Mo Alloy Steel

Bing Zheng [1,2,3], Zhipeng Zou [3,4], Dong Xu [2,3,*], Yiqun Wang [2], Xuexi Wang [2], Hongyang Zhao [1,*] and Dongying Ju [1]

1 School of Materials and Metallurgy, University of Science and Technology Liaoning, Anshan 114051, China; zhengbing1881@163.com
2 Technology Center, Henan Zhongyuan Special Steel Equipment Manufacturing Co., Ltd., Jiyuan 459008, China
3 Technology Innovation Center for High Quality Cold Heading Steel of Hebei Province, Hebei University of Engineering, Handan 056038, China
4 Technology Innovation Center for Wear Resistant Steel Plate of High Plasticity and High Toughness of Hebei Province, Hebei Puyang Iron and Steel Co., Ltd., Handan 056305, China
* Correspondence: xudong_xyz@163.com (D.X.); zhy@ustl.edu.cn (H.Z.)

Abstract: In order to study the metadynamic recrystallization behavior of 34CrNi3MoV steel, a double-pass isothermal compression experiment and a single-pass thermal interval experiment were designed and conducted to obtain the stress–strain curves under different deformation conditions and to explore the action law of deformation parameters during the compression process. The softening rate was calculated by the compensation method, and the grain size in the recrystallization region was measured. Based on the obtained data, the effects of deformation temperature (T), interval time (t), and strain rate ($\dot{\varepsilon}$) on the softening rate and grain size of 34CrNi3MoV steel during metadynamic recrystallization were analyzed. The results show that increasing the deformation temperature, extending the interval time, and increasing the strain rate are all beneficial to the improvement of the metadynamic recrystallization softening rate and that fine and uniform new grains can be obtained under a high strain rate. However, in high-temperature conditions, mixed crystallization can easily occur, which is not conducive to grain refinement. Based on the true stress–strain data and experimental data on the grain size, a relevant model for metadynamic recrystallization of 34CrNi3MoV steel was established using mathematical analysis of regression equations. The average relative error AARE between the constructed dynamic model and the grain size model and the experimental results are 6.48% and 1.30%, respectively. This indicates that the model has high predictability.

Keywords: Cr-Ni-Mo steel; metadynamic recrystallization; softening rate; kinetics models; grain size

check for updates

Citation: Zheng, B.; Zou, Z.; Xu, D.; Wang, Y.; Wang, X.; Zhao, H.; Ju, D. Metadynamic Recrystallization Behavior of Cr-Ni-Mo Alloy Steel. *Metals* **2023**, *13*, 696. https://doi.org/10.3390/met13040696

Academic Editor: Angelo Fernando Padilha

Received: 16 February 2023
Revised: 28 March 2023
Accepted: 31 March 2023
Published: 3 April 2023

1. Introduction

34CrNi3MoV steel has excellent comprehensive mechanical properties and is widely used in the manufacture of tank guns, artillery hulls, autoclaves, and other components, which are made by forging. During the forging process, when the deformation parameters and strain variables meet the dynamic recrystallization critical characteristic conditions, the material undergoes dynamic recrystallization, and the new grains after nucleation produce an internal softening effect, which effectively improves the plastic processing performance and, at the same time, refines the grains, eliminates the mixed crystals, and controls the microstructure and mechanical properties of the final material [1–6]. However, forging is limited by the loading equipment during the forging process and cannot reach the design's required deformation through a single deformation, so in the actual process, forgings often need to undergo multiple deformations to reach the final design specifications. During the multiple deformation transitions of the forging, the forgings are still in a high-temperature environment internally, with enough driving force to make the recrystallization behavior still occur inside the material, i.e., metadynamic recrystallization behavior occurs during the interval of forging. The metadynamic recrystallization behavior still has an important influence on the grain size and tissue evolution of the material [7–11].

In recent years, many scholars have conducted numerous studies on the metadynamic recrystallization behavior of different alloys using compression experiments. Zhang et al. [12] conducted a double-pass compression experiment using Ni-Cr-Mo alloy to systematically investigate the metadynamic recrystallization behavior and establish a relevant mathematical model and indicated that the metadynamic recrystallization grain size is mainly determined by the deformation temperature and strain rate during the forging process, while the results are minimally affected by the strain and initial grain size. Chen et al. [13] studied and analyzed GH738 alloy steel and concluded that the effect of prestrain on metadynamic recrystallization was obvious and pointed out that the volume fraction of metadynamic recrystallization increased and then decreased with the increase in prestrain during the double-pass compression process. Niu et al. [14] studied GH738 alloy and concluded that smaller grains can be used to increase the subdynamic recrystallization volume fraction, while extending the interval time can effectively improve the homogeneity of the forging microstructure, and increasing the strain rate of the compression process is more conducive to refining the grains and reducing the occurrence of mixed crystals. Current research on 34CrNi3MoV steel is mainly focused on the heat treatment process [15,16], while the study of recrystallization behavior during the thermal deformation process is rarely studied. The authors of the paper studied the dynamic recrystallization of 34CrNi3MoV steel in their previous work, established a corresponding model, and obtained the dynamic recrystallization critical model as $\varepsilon c = 9.57 \times 10^{-4} Z^{0.1503}$, where Z is the Zener–Hollomon parameter, which is related to the deformation temperature and strain rate.

Therefore, based on the experimental results of dynamic recrystallization of 34CrNi3MoV steel, the metadynamic recrystallization during the interval time after dynamic recrystallization was studied in this paper. A double-pass isothermal compression test was designed and carried out. The metadynamic recrystallization softening rate under various deformation process parameters was calculated using the flow stress data obtained in the experiment, and a metadynamic recrystallization dynamic model was established. In addition, in order to analyze the influence of process parameters on the evolution of metadynamic recrystallization grains, a single-pass isothermal compression post-holding test was carried out, and the grain morphology of samples after the test was observed and analyzed. Based on this, a metadynamic recrystallization grain size model of 34CrNi3MoV steel was established.

2. Experiment

The material used for the experimental specimen was 34CrNi3MoV steel, the chemical composition of which is shown in Table 1; the ingot was forged into a bar of Φ100, the sample was taken at the same position of the subsurface layer of the bar (20 mm from the surface), and the compressed specimen was machined to Φ8 mm × 12 mm using a wire cutter. The process diagram is shown in process A in Figure 1. The specimen was heated under the effect of resistance at 20 °C/s to raise the temperature of the specimen to 1200 °C, holding for 180 s to ensure the complete austenitization of the specimen and then at 10 °C/s to lower the temperature to the deformation temperature (T) (1000, 1100, 1200 °C), holding for 30 s to ensure the uniform temperature distribution of the specimen, after which the first compression test was started at a constant strain rate ($\dot{\varepsilon}$) (0.01, 0.1, 1, 5 s^{-1}) to complete the first compression experiments; the strain of compression (ε_1) was 0.4, immediately unloaded, and after an interval of time (t) (1, 5, 10, 50 s), the second compression was completed with the same deformation parameters as the first pass; the strain of compression (ε_2) was 0.4. Finally, the compression experiment was completed. In addition, we designed a single-pass post-compression holding experiment, as shown in process B in Figure 1. The preliminary process settings were kept the same as in process A.

After completing the holding gap time, the test was immediately ended, and the specimens were quenched with water to retain the austenite tissue. After the test, the specimen was cut in the extended axial direction, ground and polished, and etched with saturated aqueous picric acid solution + detergent + hydrochloric acid prepared with a certain ratio, and; finally, the compressed specimens were quenched with water, and the compressed grain morphology was observed by metallurgical microscopy (Olympus).

Table 1. Chemical composition of 34CrNi3MoV steel (%, mass fraction).

C	Si	Mn	Cr	Ni	Mo	V	Cu	P	S
0.3	0.25	0.65	1.4	3.1	0.4	0.15	≤0.02	≤0.015	≤0.001

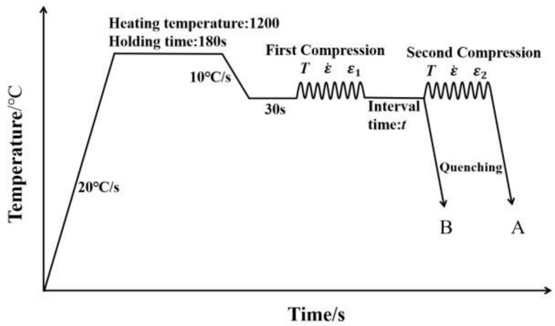

Figure 1. Experimental procedure for the isothermal interrupted hot compression experiment.

3. Results and Discussion

3.1. Flow Behavior

Figure 2 shows the flow stress curves of 34CrNi3MoV steel under different deformation temperature conditions at a strain rate of 0.01 s^{-1}. As can be seen, the curves in the figure all show peak stresses in the first pass, which is due to the fact that the strain of the first compression exceeds the critical strain of dynamic recrystallization (DRX), DRX occurs inside the material, DRX produces a softening effect and subsequently dominates the effect, and the true stress value shows a decreasing trend after the peak stress. Unloading and reloading after a certain period, the stress value appears to decrease precipitously, which is due to the continuous growth of new grains formed inside the material at high temperature during the interval time after unloading, i.e., metadynamic recrystallization (MDRX) occurs during the interval time, which causes the dislocation density to decrease rapidly and produces a more obvious softening effect. Comparing the yield stresses of the first and second passes, as can be seen, the second pass is significantly higher than the first pass, which is due to the fact that during the first compression process, the plastic deformation of the material makes the internal dislocation density of the grains increase and produces a certain amount of work hardening, resulting in an increase in the deformation resistance of the material. At the same time, with the extension of the interval time, the yield stress of the second pass decreases more obviously, indicating that the longer the interval time after unloading, the more favorable the occurrence of MDRX.

Figure 3 shows the flow stress curves of 34CrNi3MoV steel at different strain rates at a deformation temperature of 1000 °C. As can be seen, the first compression strain was 0.4 (when the deformation condition was 1000 °C and 10 s^{-1}, the DRX critical strain of 34CrNi3MoV steel was 0.305), and DRX occurred in all the materials. In Figure 3a, peak stress appears for the first time, while no peak stress appears in the curves in Figure 3b–d. This is because flow stress is the result of competition between the softening mechanism and the hardening mechanism. When DRX starts to occur, the softening effect does not offset the work of the hardening effect, and the stress still increases with the increase in strain. When the softening effect of DRX exceeds the work hardening effect, the stress will decrease with the increase in strain. As shown in Figure 3a, under the compression conditions with a strain rate of 0.01 s^{-1} and an interval time of 1 s, there is almost no work hardening in the second compression; however, with the extension of the interval time, the work hardening phenomenon becomes more and more obvious, and when the interval time reaches 50 s, the work hardening produced by the second compression is basically close to the work hardening produced by the first compression. This is due to the fact that when the interval time is very short, the new grains do not have time to grow, and the dislocation density in the crystal remains basically unchanged. With the extension of the interval time, the new grains grow gradually, the MDRX degree deepens, and a large number of dislocations is consumed such that their density decreases rapidly, which makes the first work hardening effect disappear gradually. The comparison of the curves shows that the strain rate has a great influence on the work hardening with all other parameters being the same, and the work hardening produced by high strain rate compression is more obvious in the second pass. This is due to the fact that the higher strain rate takes less time to complete the same strain during the compression process, the dislocation proliferation and stacking generated during the compression process is too late to migrate, the dislocation density increases rapidly, and the work hardening is more obvious.

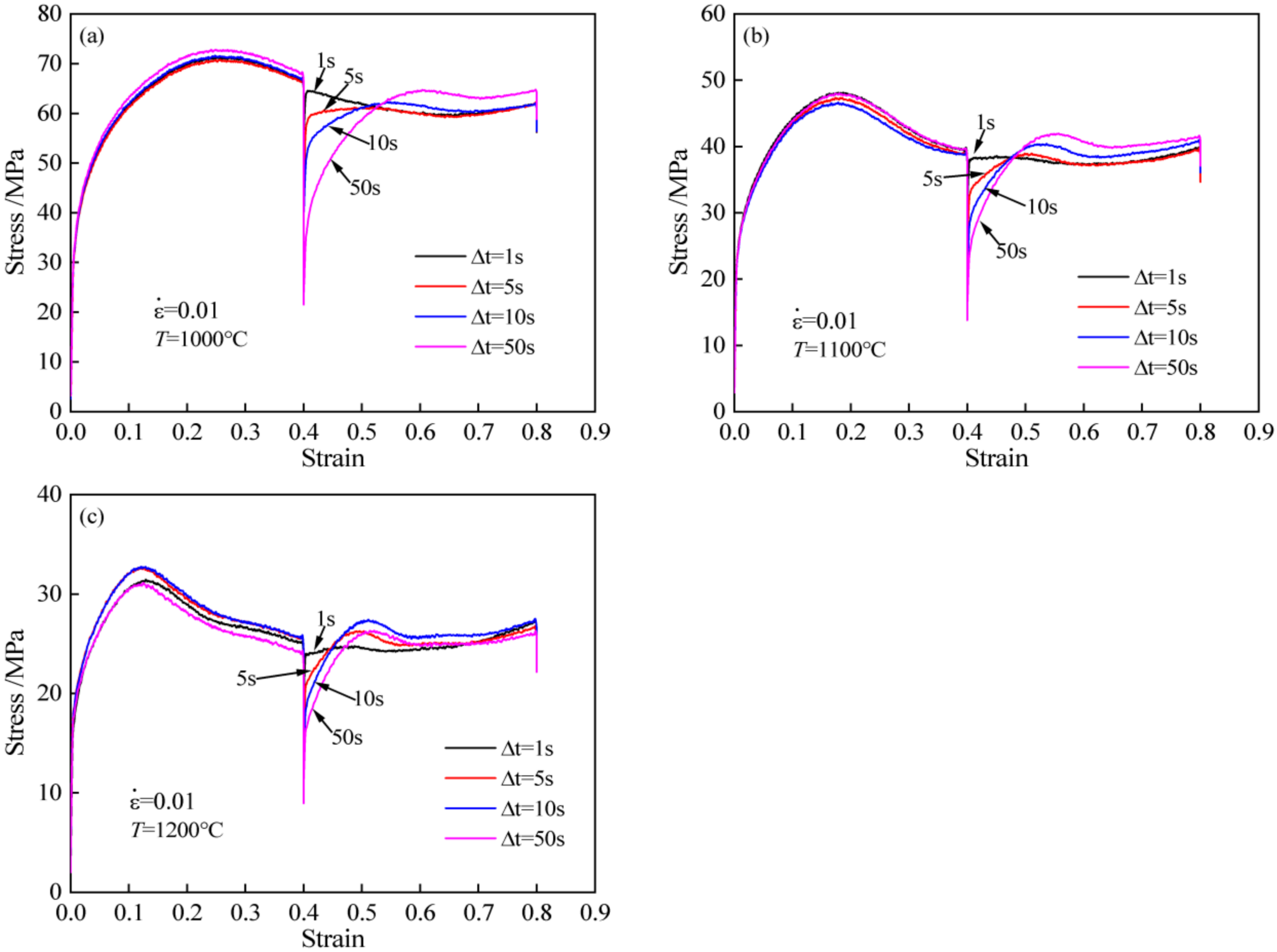

Figure 2. Flow stress curves at a strain rate of 0.01 s^{-1} under different deformation temperatures: (**a**) 1000 °C, (**b**) 1100 °C, and (**c**) 1200 °C.

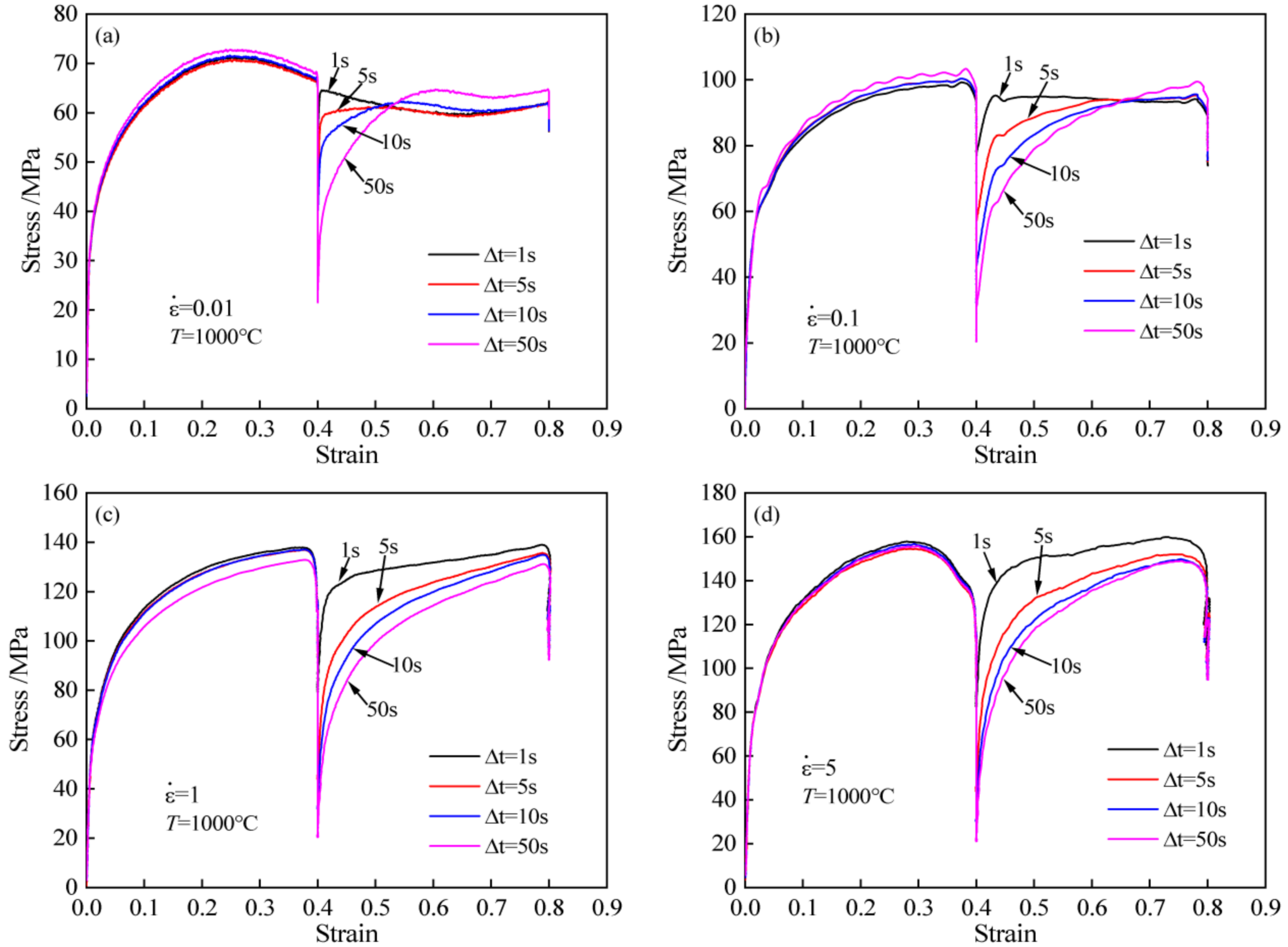

Figure 3. Flow stress curves under different strain rates at a deformation temperature of 1000 °C for (**a**) 0.01 s^{-1}, (**b**) 0.1 s^{-1}, (**c**) 1 s^{-1}, and (**d**) 5 s^{-1}.

3.2. Effect of Process Parameters on the Metadynamic Recrystallization Softening Rate and Grain Size of 34CrNi3MoV Steel

The flow stress profile changes significantly when the material undergoes MDRX during the interval of the holding time after thermoplastic deformation. The softening rate of MDRX can usually be calculated using the stress compensation method [17], the expression of which can be described by Equation (1) as follows:

$$X_{\mathrm{MDRX}} = \frac{\sigma_m - \sigma_2}{\sigma_m - \sigma_1} \quad (1)$$

where X_{MDRX} is the metadynamic recrystallization softening rate; σ_m is the stress unloaded at the end of the first pass; and σ_1 and σ_2 are the yield stresses in compression in the two passes, respectively, and the yield stress is taken as the flow stress at 0.2% strain for this calculation.

3.2.1. Effect of Deformation Temperature and Interval Time on Metadynamic Recrystallization Softening Rate and Grain Size

Figure 4 shows the curves of the law of X_{MDRX} variation with the pass interval time for 34CrNi3MoV steel under different deformation temperature conditions. Among them, Figure 4a–d have the same variation law, and Figure 4a is used as an example for analysis in this paper. The X_{MDRX} of 34CrNi3MoV steel was increased from 16.1% to 31.1% when the deformation temperature was increased from 1000 °C to 1200 °C at a strain rate of 0.01 s^{-1}

and a holding time of 1 s. The X_{MDRX} of 34CrNi3MoV steel was increased from 16.1% to 70.9% when the interval time was extended from 1 s to 50 s at a strain rate of 0.01 s^{-1} and a deformation temperature of 1000 °C. This indicates that both elevated deformation temperature and extended interval time are favorable for the increase in X_{MDRX}. This is due to the fact that the higher temperature during the intermittent time of the double-pass compression results in a higher thermal activation energy inside the material, which provides a greater driving force for the MDRX [18], while the longer intermittent time also creates conditions for the growth of new grains, and the interaction between the two results in an increase in the X_{MDRX}.

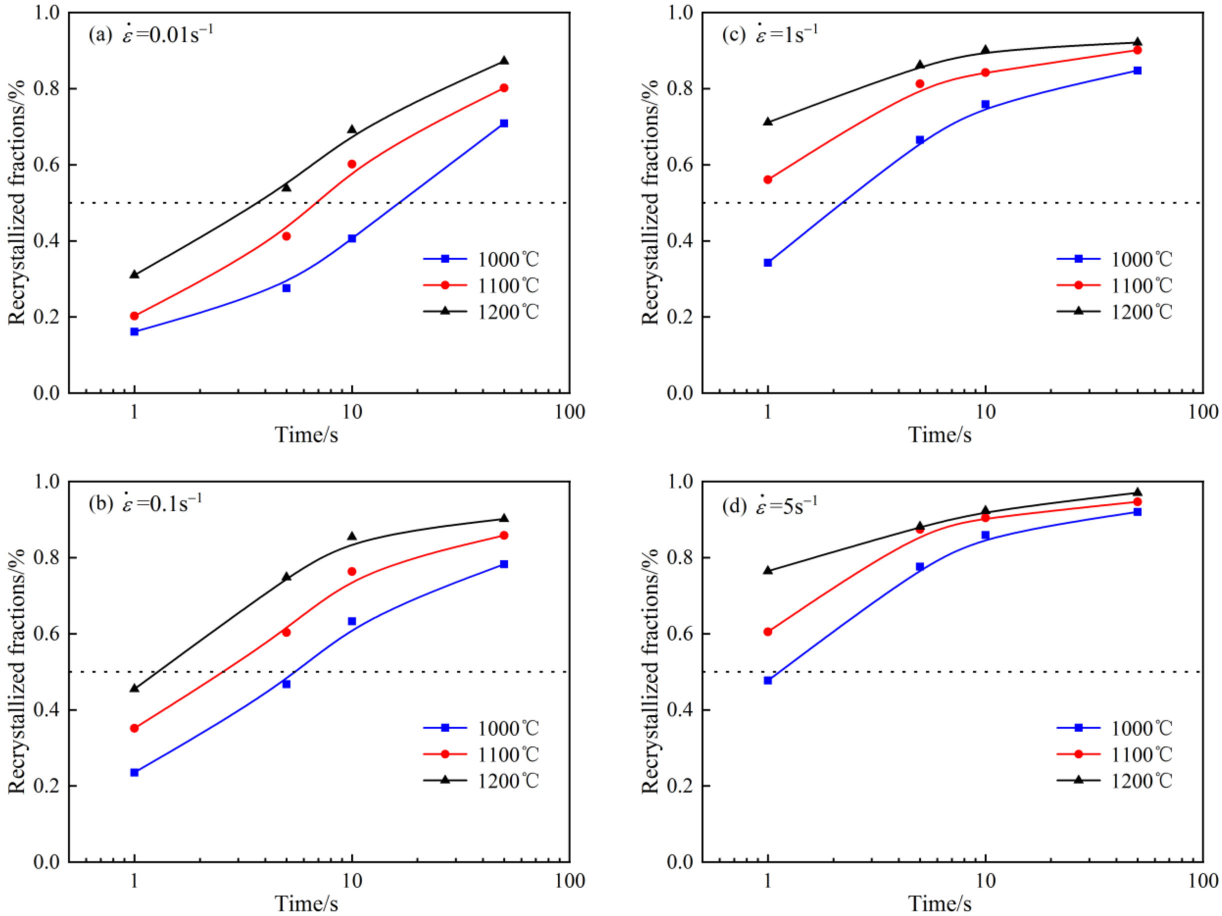

Figure 4. Variation curve of X_{MDRX} with interval time at different temperatures at different strain rates (**a**) 0.01 s^{-1}; (**b**) 0.1 s^{-1}; (**c**)1 s^{-1}; and (**d**) 5 s^{-1}.

Figure 5 shows the microstructure of the specimens after single-pass compression with a strain rate of 0.1 s^{-1}; a holding time of 5 s; and deformation temperatures of 1000, 1100, and 1200 °C. The large grains are dynamic recrystallization grains during the first compression process, and the small grains are the result of metadynamic recrystallization that occurs during the interval time. In Figure 5b,c, the dynamic recrystallization of large grains gradually decreases, the metadynamic recrystallization of small grains gradually increases, and the metadynamic recrystallization of grains tends to increase as the temperature increases. The area where recrystallization occurred at each temperature was measured using professional data analysis software, the dynamic recrystallization (large size grains) was removed during the statistical process, and the average grain size at each deformation temperature was calculated to be 17, 26, and 38 μm, respectively, based on each grain size. The grain size results indicate that the decrease in deformation temperature during double-pass compression is beneficial to grain refinement. This is due to the fact that at a lower temperature (1000 °C), dislocation migration is limited by grain boundaries, which restricts the grain growth after nucleation, as shown in Figure 5a, where the new grain size can be seen to be smaller. At a higher temperature (1200 °C), the dislocation migration process is hindered by grain boundaries, which results in faster growth of the nucleated grains, as shown in Figure 5c, where the new grain size is larger than that in Figure 5a.

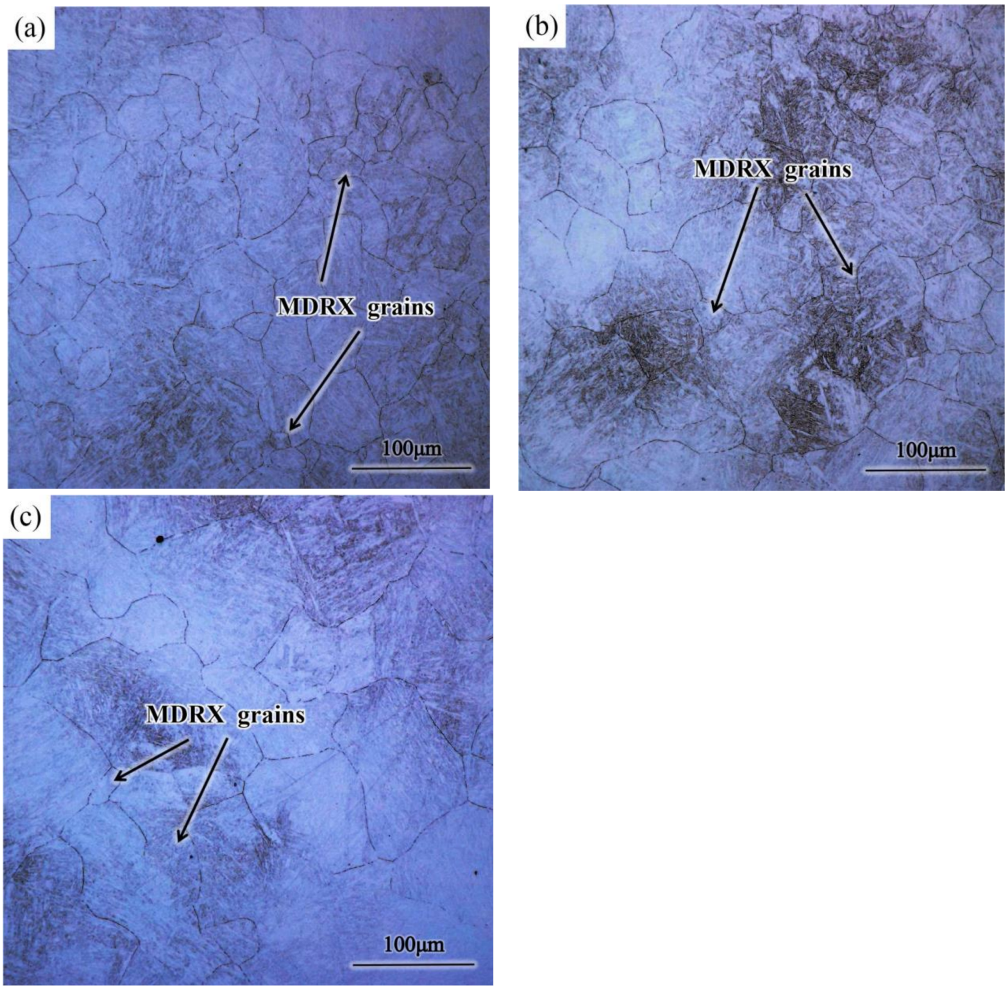

Figure 5. Grain microstructures of 34CrNi3MoV steel compressed at different temperatures. (**a**) 1000 °C, (**b**) 1100 °C, (**c**) 1200 °C ($\dot{\varepsilon}$ = 0.1 s^{-1}, t = 5 s).

Figure 6 shows the microstructure morphology of 34CrNi3MoV steel specimens after single-pass compression post holding tests at 1100 °C with a strain rate of 0.1 s^{-1} and holding times of 1, 5, 10, and 50 s. It can be seen that subdynamic recrystallization occurred in the specimens under each deformation condition. The XMDRX was calculated by Equation (1) to be 35.2%, 60.3%, 76.4%, and 85.8%, respectively. It can be seen that the softening rate of the material increases continuously, and the softening degree deepens gradually by extending the holding time between two passes. The average grain size of MDRX in the recrystallization region was calculated to be 23, 26, 30, and 38 μm. In addition, it can be seen from Figure 6a that when the holding time is 1 s, there are no "flattened and elongated" original grains, i.e., the material is completely compressed in a single pass. The DRX is consistent with the results of the previous work. In Figure 6a, the formation of MDRX fine grains distributed in the DRX grain boundaries can also be found, but the number of small grains is low, indicating that the degree of MDRX is not high; however, with extension of the casual insulation gap time, fine grains gradually increased, and the degree of MDRX gradually deepened. With an insulation time of 50 s, as shown in Figure 6d, new MDRX grains gradually increased; the grain is also more uniform than at 1 s, which is because under the deformation conditions after the compression of the insulation time, with the growth of austenite grains, grain boundaries continue to flatten, and the grain size gradually closes to the shape and tends to stabilize.

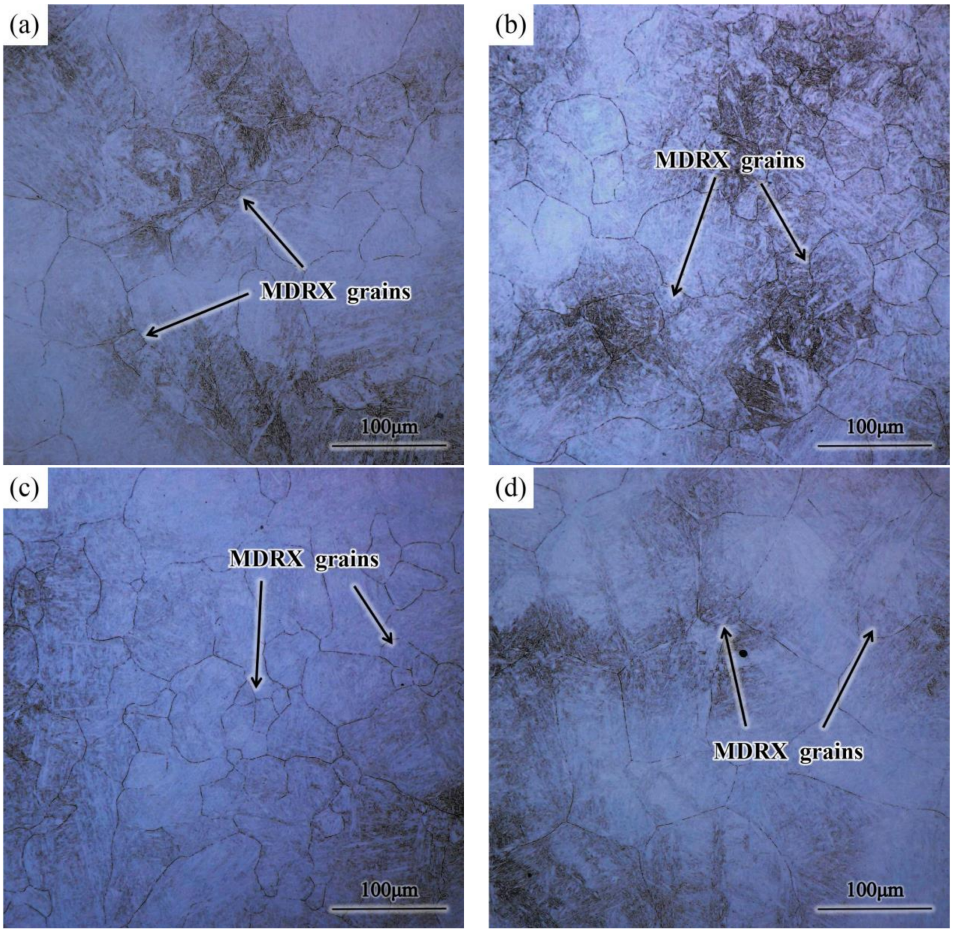

Figure 6. Grain microstructures of 34CrNi3MoV steel compressed at different intermittent times: (**a**) 1 s, (**b**) 5 s, (**c**) 10 s, and (**d**) 50 s (T = 1100 °C, $\dot{\varepsilon}$ = 0.1 s^{-1}).

3.2.2. Effect of Strain Rate on Metadynamic Recrystallization Softening Rate and Grain Size

Figure 7 shows the curves of the law of X_{MDRX} variation with the pass interval time for 34CrNi3MoV steel under different strain rate conditions. The X_{MDRX} of 34CrNi3MoV steel was increased from 30.9% to 76.5% when the strain rate was increased from 0.01 s^{-1} to 5 s^{-1} at a temperature of 1200 °C and an interval time of 1 s. As can be seen from the figure, when the deformation temperature and interval time are the same, increasing the strain rate can be beneficial to the improvement of X_{MDRX}. This is due to the shorter time required to complete the same strain at a higher strain rate during compression, which leads to a rapid increase in dislocation density at grain boundaries and a consequent increase in storage energy, providing a higher driving force for the growth of new grains of MDRX [19].

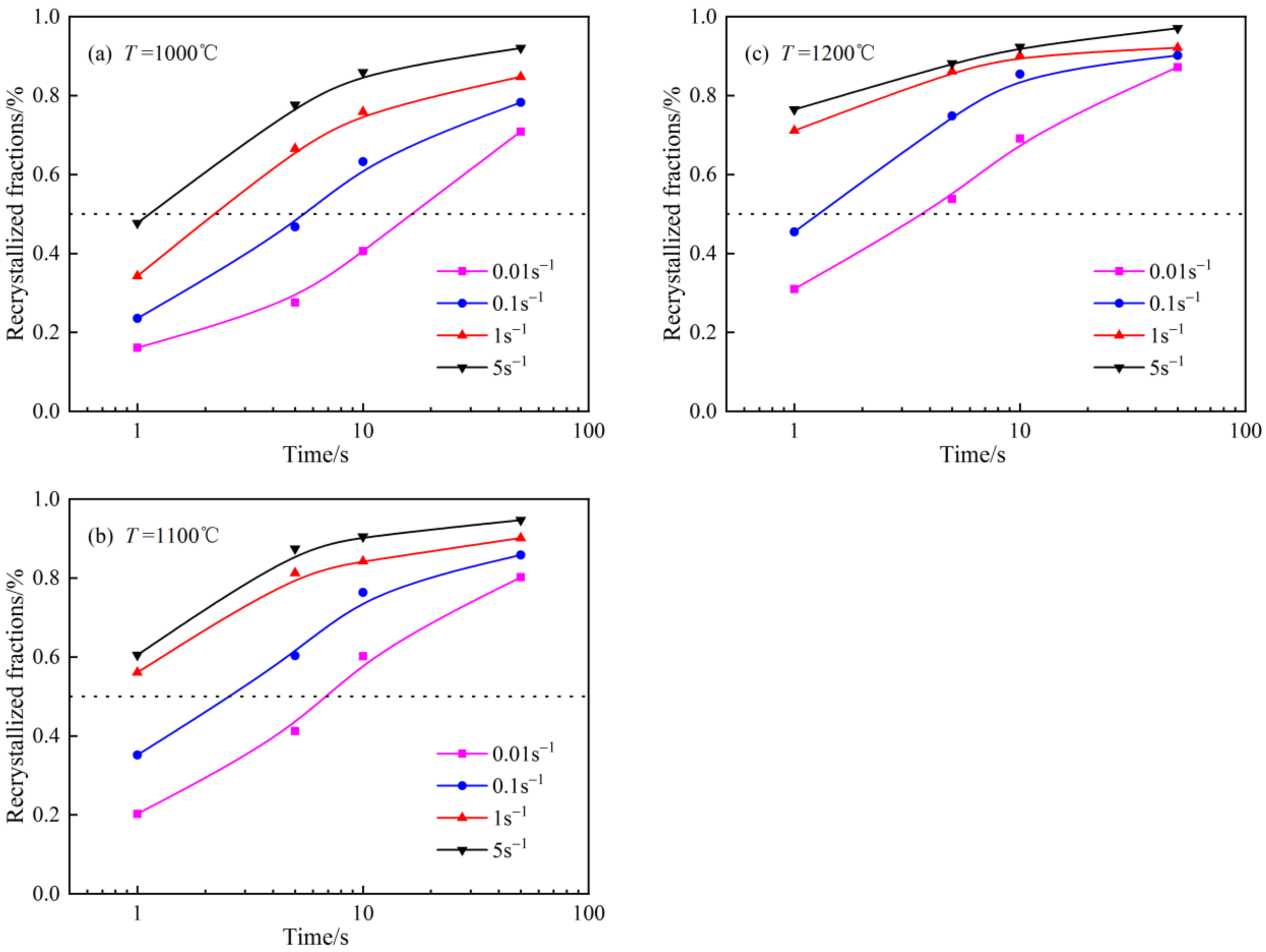

Figure 7. Variation curve of X_{MDRX} with interval time at different strain rates at different temperatures (**a**) 1000 °C; (**b**) 1100 °C; and (**c**) 1200 °C.

Figure 8 shows the microstructure of the 34CrNi3MoV steel specimens after single-pass compression and holding tests at 1100 °C; 5 s of pass holding time; and strain rates of 0.01, 0.1, 1, and 5 s^{-1}. It can be seen that subdynamic recrystallization occurred in the specimens under each deformation condition. The grain sizes in the recrystallized region were measured, the large dynamically recrystallized grains were removed during the statistical process, and the average grain sizes at each strain rate were calculated to be 29, 26, 25, and 23 μm, respectively. The grain size results indicate that finer new grains were obtained by single-pass thermal interval testing at high strain rates. This is due to the fact that during thermal deformation of the material, dislocations are subjected to stress to migrate to the grain boundaries and form dislocation buildup, which drives the recrystallization behavior. Under high strain rates, the dislocations inside the grains proliferate at a faster rate, causing the nucleation rate at the grain boundaries to increase. During the interval, the nucleated grains are limited to each other during the growth process, eventually resulting in a small grain size. In addition, compression under high-strain-rate conditions facilitates the reduction in grain size differences and improves the homogeneity of the organization. Figure 8a shows the grain morphology after compression at a strain rate of 0.01 s^{-1}. It can be seen that a small number of new grains is distributed around the original grains of very large size, and there is a significant difference between the two sizes. This is due to the fact that the new grains of small size preferentially nucleate and grow at the grain boundaries of the original grains, but the driving force is not sufficient, and the new grains grow slowly, which eventually causes a large difference in grain size.

When the strain rate is 5 s^{-1}, as shown in Figure 8d, the size difference between the original and new grains is not significant, which is due to the high strain rate of the new grains after nucleation, causing a higher driving force and gradual growth by consuming the original grains, so the final grain size tends to be uniform.

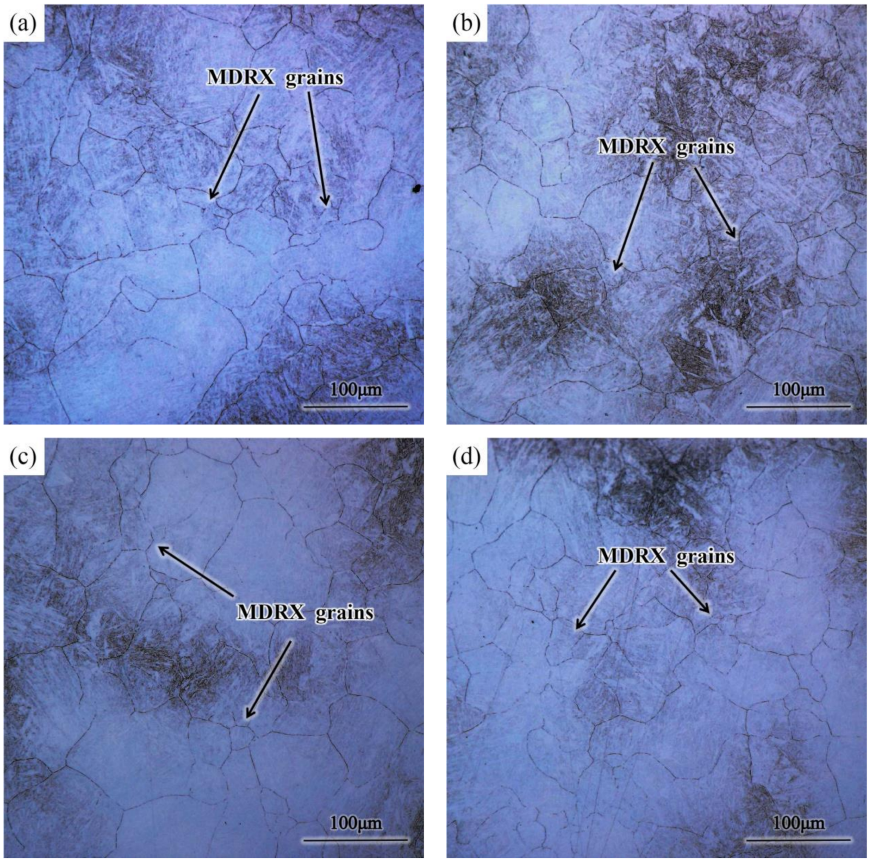

Figure 8. Grain microstructures of 34CrNi3MoV steel compressed at different strain rates: (**a**) 0.01 s^{-1}, (**b**) 0.1 s^{-1}, (**c**) 1 s^{-1}, and (**d**) 5 s^{-1} (T = 1100 °C, t = 5 s).

3.3. Establishment of Metadynamic Recrystallization Model for 34CrNi3MoV Steel

The MDRX kinetic model is usually described using the Avrami equation as follows [20]:

$$X_{\mathrm{MDRX}} = 1 - \exp\left[-0.693\left(\frac{t}{t_{0.5}}\right)^{n}\right] \tag{2}$$

where t is the interval time, n is the material parameter, and $t_{0.5}$ is the time at which X_{MDRX} is 50%.

3.3.1. Determination of $t_{0.5}$ Formula

Figures 4 and 7 show the curves of X_{MDRX} with the interval time (t) under different deformation parameters, and the time when X_{MDRX} is 50% can be obtained; the statistical results are shown in Table 2.

$t_{0.5}$ is related to both deformation temperature and strain rate and is generally described using Equation (3) as follows [21]:

$$t_{0.5} = a\dot{\varepsilon}^{m} \exp\left(\frac{Q_{\mathrm{MDRX}}}{RT}\right) \tag{3}$$

where a and m are material parameters, T is the absolute temperature, Q_{MDRX} is the activation energy of MDRX (J/mol), and R is the gas constant (8.314 J/(mol·K)).

Table 2. $t_{0.5}$ of 34CrNi3MoV steel under different deformation conditions.

Deformation Temperature (°C)	Strain Rate (s^{-1})	$t_{0.5}$ (s)
1000	0.01	16.42
1000	0.1	5.54
1000	1	2.28
1000	5	1.13
1100	0.01	6.88
1100	0.1	2.53
1200	0.01	3.66
1200	0.1	1.29

In order to determine the values of the activation energy (Q_{MDRX}) and the material parameters a and m, logarithms on both sides of Equations (3) and (4) can be obtained as follows:

$$\ln t_{0.5} = \ln a + m\dot{\varepsilon} + Q_{MDRX}/RT \tag{4}$$

Partial differentiation of the deformation parameters in Equation (4) yields:

$$m = \frac{\partial(\ln t_{0.5})}{\partial\dot{\varepsilon}} \tag{5}$$

$$Q_{MDRX} = \frac{\partial(\ln t_{0.5})}{\partial(1/T)} \tag{6}$$

According to Equations (5) and (6), the data in Table 2 are substituted, and linear regression analysis is performed to obtain the slope, as shown in Figure 9; Figure 9a,b are the fitting graphs of $\ln t_{0.5} - \ln\dot{\varepsilon}$ and $\ln t_{0.5} - 1000/T$, respectively. Through the fitting slope, it is calculated that $m = -0.438$, $Q_{MDRX} = 115{,}453$ J·mol^{-1}, and $a = 3.76 \times 10^{-5}$ according to the intercept. Therefore, $t_{0.5}$ with the deformation temperature and strain rate can be expressed as:

$$t_{0.5} = 3.76 \times 10^{-5}\dot{\varepsilon}^{-0.438} \exp\left(\frac{115453}{RT}\right) \tag{7}$$

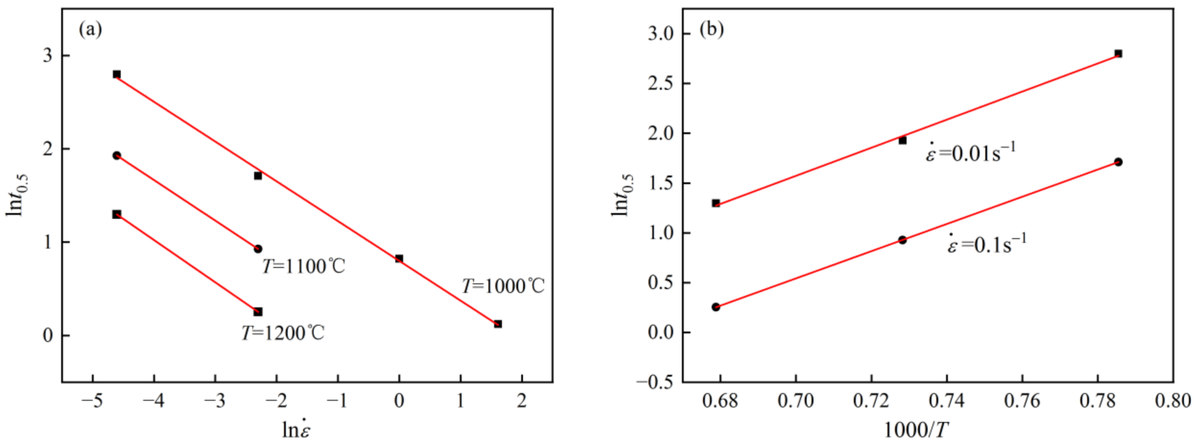

Figure 9. The relationship between ln$\dot{\varepsilon}$, 1000/T and ln$t_{0.5}$. (**a**) $\ln t_{0.5} - \ln\dot{\varepsilon}$; (**b**) $\ln t_{0.5} - 1000/T$.

3.3.2. Determination of the Dynamical Model

The MDRX kinetic equation for 34CrNi3MoV steel is usually formulated using the Avrami equation of Equation (2). In order to determine the value of the material parameter n, Equation (8) can be obtained after taking the logarithm of each side of Equation (2).

$$\ln[-\ln(1 - X_{MDRX})] = \ln 0.693 + n\ln(t/t_{0.5}) \tag{8}$$

Equation (8) shows that there is a certain linear relationship between $\ln[-\ln(1 - X_{MDRX})]$ and $\ln(t/t_{0.5})$, and the slope of the linear fit is n. The X_{MDRX}, $t_{0.5}$, and t calculated under different deformation conditions are brought into Equation (8) with a fixed intercept of ln0.693, and a linear fit is performed as shown in Figure 10; the value of the material parameter n can be calculated as 0.419 according to the fitted slope, where the fitted correlation coefficient is R^2 = 0.95.

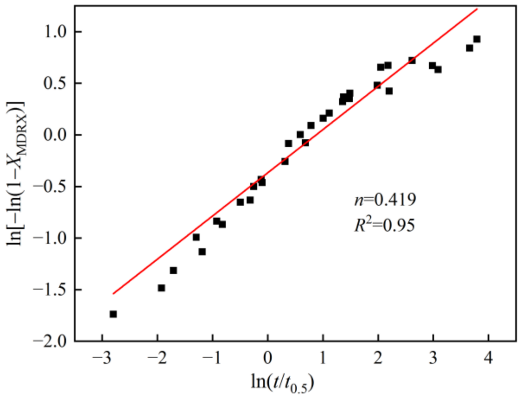

Figure 10. The relationship between ln $[-\ln(1-X_{MDRX})]$ and ln $(t/t_{0.5})$.

Therefore, the kinetic model for the MDRX kinetics of 34CrNi3MoV steel can be described by Equation (9) as follows.

Thus, the kinetic model for the MDRX kinetics of 34CrNi3MoV steel can be described as:

$$\begin{cases} X_{MDRX} = 1 - \exp\left[-0693\left(\frac{t}{t_{0.5}}\right)^{0.419}\right] \\ t_{0.5} = 3.76 \times 10^{-5}\dot{\varepsilon}^{-0.438}\exp\left(\frac{115453}{RT}\right) \end{cases} \quad (9)$$

3.3.3. Validation of the Model

The method of using the degree of softening to calculate X_{MDRX} (Equation (1)) has been widely used. However, the established kinetic model (Equation (9)) was fitted several times to obtain the results and verify the accuracy of the model. The kinetic model validation curve was fitted as shown in Figure 11. As can be seen, the X_{MDRX} calculated using the degree of softening is closer to the data obtained from the kinetic model, and the discrete points are basically around $y = x$, where the correlation coefficient (R^2) is 0.982, and the average relative error *AARE* is only 6.48%, indicating that the two pieces of data have a high degree of agreement and that the established kinetic model can predict X_{MDRX} in the heat deformation process very accurately.

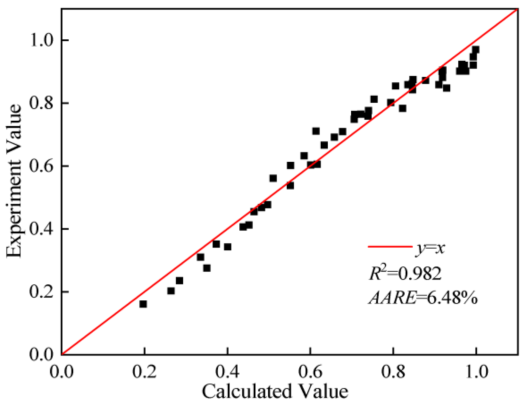

Figure 11. Validation curve of the MDRX kinetic model of 34CrNi3MoV steel.

3.4. Grain Size Equation Establishment

During metadynamic recrystallization, the deformation parameters have a significant effect on the grain size [22]. The size of the grains in the recrystallization region was measured, and the average grain size was calculated. Through the statistics of the average grain size, the evolution law of the average grain size was investigated, and the related mathematical model was established, as shown in Equation (10).

$$D_{\mathrm{MDRX}} = A\dot{\varepsilon}^{n}\exp(Q_2/RT) \tag{10}$$

where D_{MDRX} is the average grain size of metadynamic recrystallization; A and n are the material parameters, respectively; and Q is the activation energy (kJ·mol^{-1}).

In order to determine the values of the material parameters A, n, and Q_2, taking logarithms on both sides of Equation (10), Equation (11) can be obtained as follows:

$$\ln D_{\mathrm{MDRX}} = \ln A + n\ln\dot{\varepsilon} + Q_2/RT \tag{11}$$

Partial differentiation of the deformation parameters in Equation (11) yields:

$$n = \frac{\partial \ln D_{\mathrm{MDRX}}}{\partial \ln\dot{\varepsilon}},\ Q_2 = R\frac{\partial \ln D_{\mathrm{MDRX}}}{\partial(1/T)} \tag{12}$$

By fitting a linear fit between $\ln D_{\mathrm{MDRX}}$ and $\ln\dot{\varepsilon}$ and $1000/T$, as shown in Figure 12, Figure 12a,b are the fitting graphs of $\ln D_{\mathrm{MDRX}} - \ln\dot{\varepsilon}$ and $\ln D_{\mathrm{MDRX}} - T/1000$, respectively. n = -0.035 and Q_2 = $-62{,}689$ were obtained using the slope, and A = 5845 was obtained according to the intercept in Figure 12b.

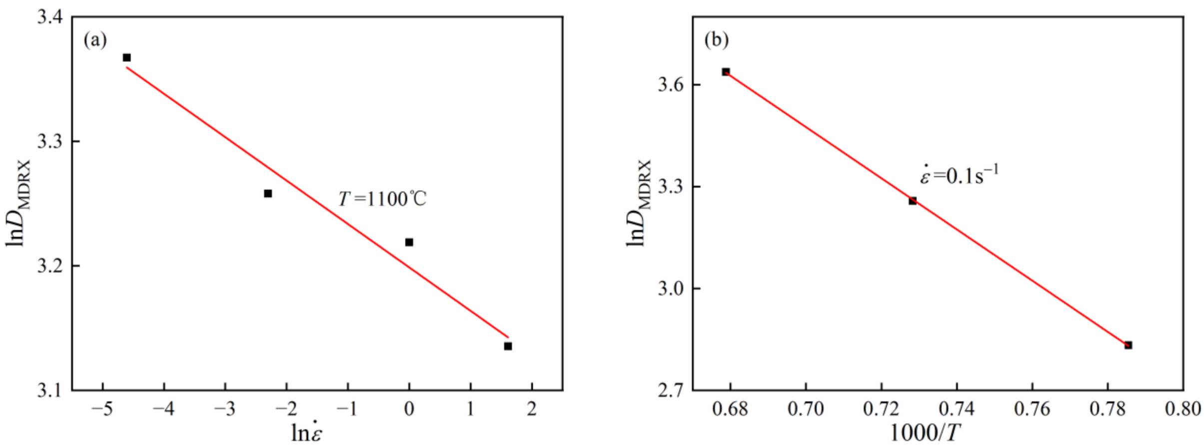

Figure 12. The relationship between $\ln\dot{\varepsilon}$, $1000/T$ and $\ln D_{\mathrm{MDRX}}$. (**a**) $\ln D_{\mathrm{MDRX}} - \ln\dot{\varepsilon}$; (**b**) $\ln D_{\mathrm{MDRX}} - 1000/T$.

The D_{MDRX} model for 34CrNi3MoV steel was obtained by substituting the calculated parameters of each material into Equation (10), which can be described by Equation (13) as follows:

$$D_{\mathrm{MDRX}} = 62770\dot{\varepsilon}^{-0.107}\exp(-92860/RT) \tag{13}$$

Figure 13 shows the validation curve of the D_{MDRX} model for 34CrNi3MoV steel, and the discrete points are basically around $y = x$, where the correlation coefficient (R^2) is 0.998, and the average relative error *AARE* is only 1.30%, indicating that the two data points have a high degree of agreement and that the grain size model can very accurately predict D_{MDRX} in the heat deformation process.

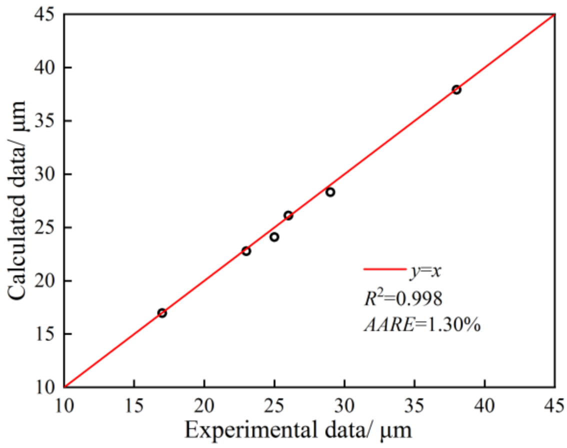

Figure 13. Verification curve of MDRX average grain size of 34CrNi3MoV steel.

4. Conclusions

The MDRX behavior of 34CrNi3MoV steel was investigated by hot compression experiments, of which the main conclusions can be summarized as follows:

(1) Increasing the deformation temperature, extending the interval time, and increasing the strain rate are all beneficial to the improvement of the metadynamic recrystallization softening rate, and fine and uniform new grains can be obtained under a high strain rate. However, in high-temperature conditions, mixed crystallization can easily occur, which is not conducive to grain refinement.

(2) The MDRX kinetic model for 34CrNi3MoV steel can be described as:

$$\begin{cases} X_{\mathrm{MDRX}} = 1 - \exp\left[-0.693\left(\frac{t}{t_{0.5}}\right)^{0.419}\right] \\ t_{0.5} = 3.76 \times 10^{-5}\dot{\varepsilon}^{-0.438}\exp\left(\frac{115453}{RT}\right) \end{cases}$$

(3) The MDRX grain size model for 34CrNi3MoV steel can be described as:

$$D_{\mathrm{MDRX}} = 62770\dot{\varepsilon}^{-0.107}\exp(-92860/RT)$$

Author Contributions: Methodology, B.Z. and D.X.; Investigation, Z.Z. and X.W.; Validation, Y.W.; Writing—original draft preparation, B.Z.; Writing—review and editing, D.X.; Supervision, H.Z. and D.J.; Funding acquisition, D.X. All authors have read and agreed to the published version of the manuscript.

Funding: This research was funded by the National Natural Science Foundation of China (NSFC) (U20A20272), Special Projects for Military–Civilian Collaborative Innovation in Science and Technology of Hebei Province (22351001D), a key project of the Handan Scientific Research Program (21122015004), and the Science and Technology Project of the Hebei Education Department (CXY2023004).

Data Availability Statement: The data that support the findings of this study are available from the corresponding author upon reasonable request.

Conflicts of Interest: The authors have no conflict of interest to disclose.

References

1. Liu, Z.G.; Li, P.J.; Yin, X.Y.; Wu, F.Y.; Xiong, L.T.; Gao, H.T. Effects of Deformation Parameters on the Superplastic Behavior and Microstructure Evolution of TA32 Alloy. *Rare Met. Mater. Eng.* **2018**, *47*, 3473–3481.
2. Lei, L.; Yang, Q.B.; Zhang, Z.Q.; Fan, X.Z.; Li, X.; Yang, M.; Deng, Z.H. Multi-pass Compression Behavior and Microstructure Evolution of AA2195 Aluminum Lithium Alloy. *Mater. Rep.* **2019**, *33*, 348–352.

3. Gan, H.Y.; Cheng, M.; Song, H.W.; Chen, Y.; Zhang, S.H.; Vladimir, P. Dynamic Recrystallization and texture evolution of GH4169 alloy during cross wedge rolling. *J. Mater. Eng.* **2020**, *48*, 114–122.
4. Qiao, S.B.; He, X.K.; Liu, J.J.; Zhao, D.L.; Liu, Z.D. Microstructure evolution and flow stress modeling of SA508Gr.4N steel during hot deformation process. *J. Mater. Eng.* **2021**, *49*, 67–77.
5. Pan, L.B.; Chu, T.; Zhang, S.; Jiang, J.; Cheng, C.J.; Xie, Q.Z.; Xing, X.Q.; Si, T.Z. Dynamic recrystallization behaviors of 30CrNi3MoV steel and its mathematical models. *Heat Treat. Met.* **2021**, *46*, 23–30.
6. Wu, C.H.; Feng, D.; Zang, Q.H.; Fan, S.C.; Zhang, H.; Li, Y.S. Microstructure Evolution and Recrystallization Behavior During Hot Deformation of Spray Formed AlSiCuMg Alloy. *Acta Metall. Sin.* **2022**, *58*, 932–942.
7. Zhao, M.J.; Huang, L.; Zeng, R.; Su, H.L.; Wen, D.X.; Li, J.J. In-situ observations and modeling of metadynamic recrystallization in 300M steel. *Mater. Charact.* **2020**, *159*, 109997. [CrossRef]
8. Shen, W.F.; Zhang, C.; Zhang, L.W.; Xia, Y.N.; Xu, Y.F.; Shi, X.H. Metadynamic recrystallization of Nb–V microalloyed steel during hot deformation. *J. Mater. Res.* **2017**, *32*, 656–665. [CrossRef]
9. Wang, Y.S.; Hu, Z.Q.; Wang, K.K.; Li, H. Investigation on meta-dynamic recrystallization behavior of 5CrNiMoV hot-working die steel. *J. Plast. Eng.* **2021**, *28*, 118–125.
10. Chen, W.X.; Hu, B.J.; Jia, C.N.; Zheng, C.W.; Li, D.Z. Post-Dynamic Softening of Austenite in a Ni-30%Fe Model Alloy After Hot Deformation. *Acta Metall. Sin.* **2020**, *56*, 874–884.
11. Ma, Q.; Wei, K.; Tang, H.B.; Dong, X.J. Softening behavior and equiaxed α phase microstructure evolution of TA15 titanium alloy during double-pass hot compression deformatiion. *Trans. Mater. Heat Treat.* **2021**, *42*, 40–47.
12. Zhang, C.; Zhang, L.W.; Shen, W.F.; Liu, C.R.; Xia, Y.N. The Kinetics of Metadynamic Recrystallization in a Ni-Cr-Mo-Based Superalloy Hastelloy C-276. *J. Mater. Eng. Perform.* **2016**, *25*, 545–552. [CrossRef]
13. Chen, X.M.; Lin, Y.C.; Li, X.H.; Chen, M.S.; Yuan, W.Q. lnvestigation on strain dependence of metadynamic recrystallization behaviors of GH4169 superalloy. *Vacuum* **2018**, *149*, 1–11. [CrossRef]
14. Niu, W.L.; Guo, J.; Ma, S.W.; Zhang, M.C. Maicang Sub-dynamic Recrystallization Kinetics Model of the New Type Alloy of High-Quality GH738. *Rare Met. Mater. Eng.* **2022**, *51*, 183–189.
15. Wang, Y.J.; Liu, Z.C.; Duan, B.Y. Microstructure of refined 34CrNi3MoV steel. *Ordnance Mater. Sci. Eng.* **2013**, *36*, 128–132.
16. Zhao, Y.T.; Liu, Z.C.; Wang, Y.F. Mixed Grain and Elimination Measure of 34CrNi3MoV Steel. *Heat Treat. Met.* **2007**, *25*, 75–77.
17. Xu, Y.; Jiao, Y.X.; Liu, J.S. Modeling of Metadynamic Recrystallization Kinetics and Recrystallization Mechanisms of V-Containing 12Cr Rotor Steel. *J. Mater. Eng. Perform.* **2020**, *29*, 4754–4765. [CrossRef]
18. Zhang, W.; Zhang, J.; Han, Y.; Liu, R.; Zou, D.N.; Qiao, G.J. Metadynamic Recrystallization Behavior of As-cast 904L Super-austenitic Stainless Steel. *J. Iron Steel Res. Int.* **2016**, *23*, 151–159. [CrossRef]
19. Cheng, Y.; Du, H.Y.; Wei, Y.H.; Hou, L.F.; Liu, B.S. Metadynamic recrystallization behavior and workability characteristics of HR3C austenitic heat-resistant stainless steel with processing map. *J. Mater. Process. Tech.* **2016**, *235*, 134–142. [CrossRef]
20. Liang, M.Q.; Li, X.X.; Zhang, Y.L.; Zhang, W.; Huang, D.C. Analysis on sub-dynamic recrystallization and establishment of mathematic model for non-quenched and tempered steel. *Forg. Stamp. Technol.* **2021**, *46*, 175–178.
21. Zhang, C.; Zhang, L.W.; Shen, W.F.; Xia, Y.N. The kinetics and microstructural evolution during metadynamic recrystallization of medium carbon Cr–Ni–Mo alloyed steel. *J. Mater. Res.* **2017**, *32*, 1367–1375. [CrossRef]
22. Liu, D.H.; Chen, J.D.; Chai, H.R.; Jiang, Y.H.; Li, Z.; Qiu, W.Q.; Guo, Z.H. Study of meta-dynamic recrystallization behavior of GH5188 superalloy. *J. Mater. Res. Technol.* **2021**, *15*, 1179–1189. [CrossRef]